Event reconstruction and neutrino selection with KM3NeT/ARCA230

Thijs Juan van Eeden[a,*] and Jordan Seneca[a] for the KM3NeT collaboration

[a]*Nikhef,*
Science Park 105, Amsterdam, Netherlands

E-mail: tjuanve@nikhef.nl

The discovery of high-energy cosmic neutrinos has raised great interest in the field of neutrino astronomy. The KM3NeT/ARCA detector is currently under construction at the bottom of the Mediterranean Sea and is measuring high-energy neutrinos. The complete detector will instrument a cubic kilometre of seawater with photomultiplier tubes that detect the Cherenkov radiation from the products of neutrino interactions. The design is focused on discovering high-energy neutrino sources which requires an excellent angular resolution. This contribution covers the reconstruction algorithms deployed in the full KM3NeT/ARCA detector and their performances. The angular resolution reaches below $0.1°$ for tracks and below $1°$ for cascades and double cascades that originate from tau neutrinos. Additionally, the neutrino selections for the full KM3NeT/ARCA diffuse and point source studies are covered.

*Speaker

1. Introduction

The detection of high energy cosmic neutrinos by IceCube accelerated the field of neutrino astronomy [1]. IceCube detected a high-energy neutrino event coincident with a gamma-ray flare from TXS 0506+056 [2] and an excess of events from nearby active galaxy NGC 1068 [3] but there are many sources yet to be discovered.

The KM3NeT/ARCA detector is currently under construction offshore from Porto Palo di Capo Passero, Sicily, Italy [4]. Its primary purpose is to detect neutrinos with energies ranging from TeV and beyond. The field of the detector view covers the Southern sky in order to study potential Galactic sources. The detector consists of a three-dimensional grid of optical modules at the bottom of the Mediterrean sea [5]. Each optical module houses 31 photomultiplier tubes (PMTs) and data acquisition hardware. Each vertical detection string contains 18 modules that are mounted to the seabed. The final detector configuration will have 230 strings covering an instrumented volume of approximately 1 km^3.

The discovery and characterisation of new neutrino sources is enabled by reconstruction and selection of neutrino and background event. This contribution covers the full detector (KM3NeT/ARCA230) reconstruction algorithms and performance for track, shower and double shower topologies. This is followed by the track and shower event selections that are used for the current point source and diffuse flux analyses.

2. Simulation

Neutrino events are simulated using the gSeaGen simulation framework [6]. All neutrino flavours and interactions are simulated with energies from 10^2 to 10^8 GeV and weighted using different flux models. The atmospheric flux consists of a conventional and prompt component as described in [7].

The atmospheric muon events are generated using parametric formulas implemented in the MUPAGE software package [8]. Two samples of atmospheric muon are generated. One with a bundle threshold of 10 TeV and one of 50 TeV to increase statistics at high energies.

The generated events are processed by software packages for the light simulation and detector response. The track and shower reconstruction are applied to all events.

3. Event reconstruction

The event reconstruction algorithms covered in this contribution are based on a maximum likelihood search method.

3.1 Track reconstruction

The track reconstruction fits the energy and direction of high-energetic muons [9]. A coordinate transformation is applied to align a muon direction hypothesis with the z-axis. The muon trajectory can then be described by 5 parameters

- ρ_i: distance of closest approach muon track with PMT,

- θ_i, ϕ_i: PMT orientation angles,

- Δt: difference between and measured and expected hit time according to the Cherenkov hypothesis,

- E: energy of the muon.

The non-linearity of the problem requires a prefit where scattering and dispersion of light is neglected. This results in a linear fit that is performed over all directions with a 1° grid angle. The best 12 fits are stored and passed to the final fit. This fit maximises the likelihood

$$\text{Likelihood} = \prod_{\text{hit PMTs}} \frac{\partial P}{\partial t}(\rho_i, \theta_i, \phi_i, \Delta t, E) \tag{1}$$

where $\frac{\partial P}{\partial t}$ is a semi-analytical probability density function (PDF) which gives the expected scattered and unscattered photons from Chrerenkov radation and energy losses of a muon. This PDF includes detector effects like the quantum efficiency and transit time spread of PMTs and background rates from K40 decays in seawater. Figure 1 shows the angular resolution of the track reconstruction for the track selection (described in section 4) ν_μCC events using the KM3NeT/ARCA230 detector. The energy resolution is defined as half the difference between the 16th and 84th percentiles of the energy bias distributions (Energy bias $= 100\% \cdot \left(\frac{E_{rec}}{E_{visible}} - 1 \right)$) and is shown in Figure 2(b).
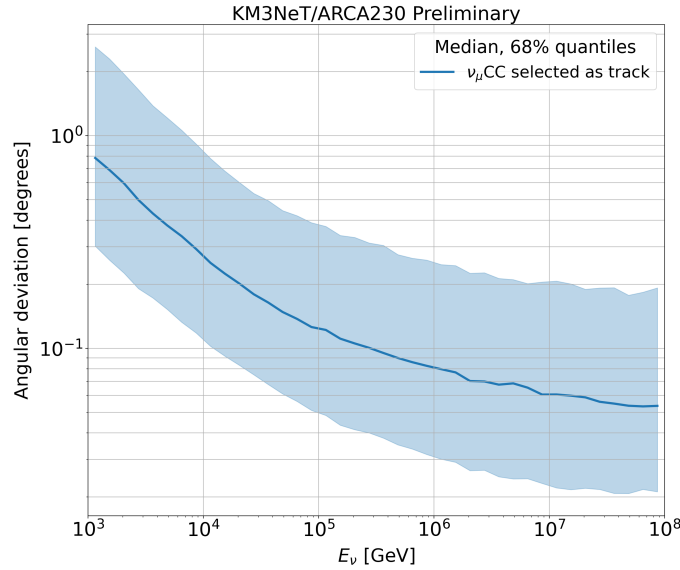

Figure 1: KM3NeT/ARCA230 angular resolution for ν_μCC of the track selection described in section 4.

3.2 Shower reconstruction

The KM3NeT/ARCA230 shower reconstruction also follows a two-step procedure [9]. The first step selects coincident hits on the same optical module within 20 ns. Subsequently the vertex

position and time is found by minimising

$$M = \sum_{i \in \text{hits}} \sqrt{1 + (t_i - \hat{t}_i)} \tag{2}$$

where t_i is the measured hit time and $\hat{t}_i$ the expected hit time assuming a spherical light pattern emitted from the vertex. The final fit tests different direction hypotheses around the fitted vertex position. Twelve isotropic starting directions are chosen where the following likelihood is maximised

$$\log L = \sum_{i \in \text{hits}} \log(P_i^{\text{hit PMTs}}) + \sum_{i \in \text{no hit PMTs}} \log(P_i^{\text{no hit}}) \tag{3}$$

$$P_i^{\text{hit}} = 1 - P_i^{\text{no hit}} = 1 - \exp(-\mu_{\text{sig}}(r_i, z_i, a_i, E) - R_{\text{bg}} \cdot T) \tag{4}$$

where μ_{sig} is obtained from interpolating a PDF based on Monte Carlo simulations and R_{bg} is expected background rate in time window T. The PDF depends on the distance from the vertex to the PMT (r_i), the angle between the neutrino direction and the vector between the vertex and the PMT (z_i), the angle between the normal vector of the PMT and the vector between the vertex and the PMT (a_i) and scales linearly with energy. The direction and energy resolution of ν_eCC events selected as shower (described in section 4) are shown in figure 2.
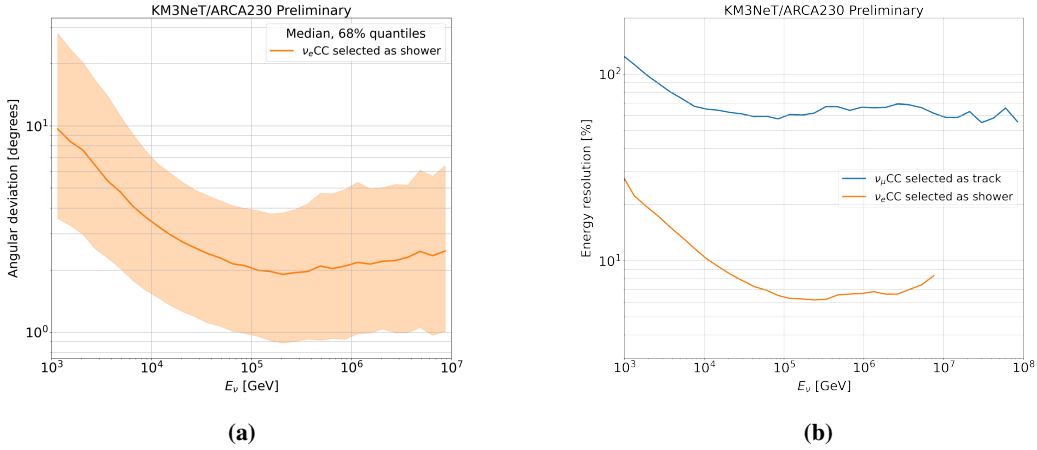

(a)
(b)

Figure 2: KM3NeT/ARCA230 angular resolution (a) for ν_eCC of the shower selection (described in section 4). The energy resolution (b) of ν_μCC selected as track and ν_eCC selected as shower.

3.3 Improvements

The shower reconstruction can be improved when including timing information in the fit procedure [10]. High-energy showers are elongated over several meters resulting in a small lever arm that helps the direction reconstruction. The algorithm is currently too computationally expensive to run over large datasets, but figure 3 (a) shows contained ν_eCC events reconstructed with and without timing information. The resolutions drops from $2°$ to below $1°$.

The inclusion of timing information in the reconstruction also opens up the door in reconstructing double shower events. These events are caused by ν_τCC interactions where the τ decays

into a electromagnetic or hadronic shower. The relativistic τ can travel approximately 5 m/100 TeV resulting in two separated showers. The double shower reconstruction fits a double shower model based on the hit time information [10]. The fit starting point is the traditional shower reconstruction result. This is followed by a prefit to get a first estimate of the first and second shower position. Finally a full fit is performed where the primary vertex, tau flight length, direction and two energies are fitted. Figure 3 (b) shows the angular resolution as a function of the tau length for contained events with $E_\nu > 100$ TeV. Dedicated tau selections and analyses are in preparation.
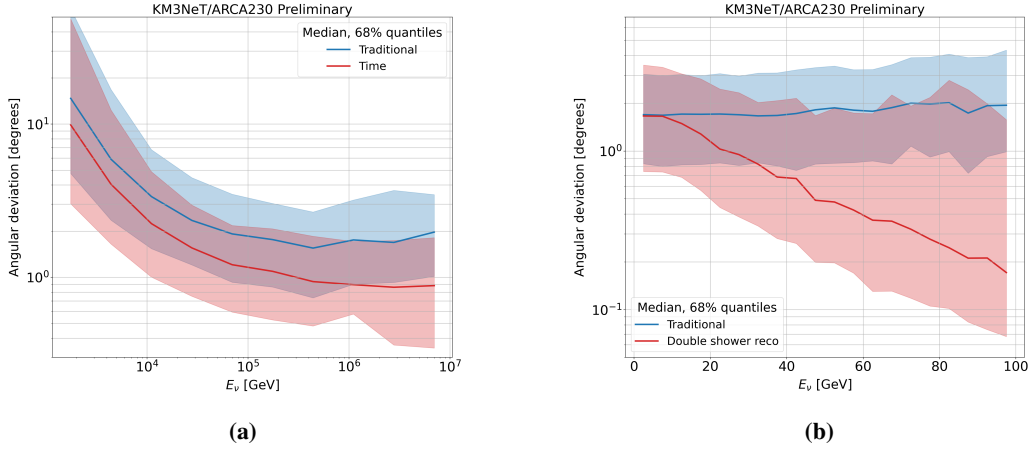

(a)   **(b)**

Figure 3: Angular resolution for the shower reconstruction with timing information (a) and the double cascade reconstruction (b). Both results are compared with the traditional shower reconstruction. The time shower reconstruction shows contained ν_eCC. The double cascade reconstruction contained ν_τCC shower decay events with $E_\nu > 100$ TeV.

4. Neutrino selections

The neutrino purity is increased by applying cuts to remove atmospheric muon events. This is done for two separate observation channels; tracks and showers. The variables used for rejecting background are output from the track and traditional shower reconstruction. Selection cuts are followed by the training of a boosted decision tree model to obtain the final selections. Selections based on the time shower fit and double cascade reconstruction are under preparation.

4.1 Track selection

The track selection is optimised to find upgoing track-like neutrino events that are reconstructed within 10° of the neutrino direction. Upgoing and horizontal events are selected for reconstructed zenith $\theta < 100°$. Various variables of these events are used to train the boosted decision tree model including reconstructed energy, fit quality, direction error, track length and more. The final selection contains a more strict cut for horizontal ($80° < \theta < 100°$) events due to higher mis-reconstructed muon contamination. Figure 4 shows the KM3NeT/ARCA230 event rate per year versus the reconstructed energy and zenith of the track selection for a cosmic neutrino flux of $\phi_{\nu_i + \bar{\nu}_i} = 1.2 \cdot 10^{-8} \left(\frac{E_\nu}{\text{GeV}} \right)^{-2} \text{GeV}^{-1} \text{ cm}^{-2} \text{ s}^{-1} \text{ sr}^{-1}$.
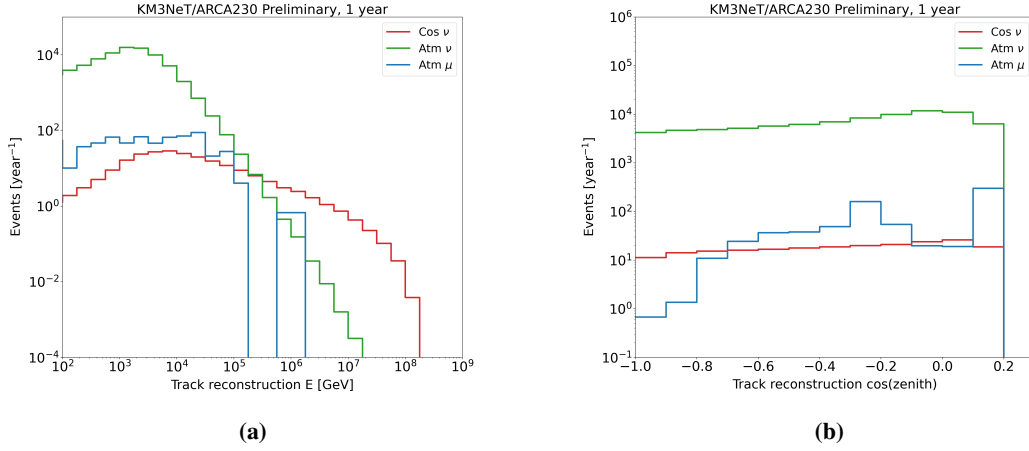
(a)

(b)

Figure 4: KM3NeT/ARCA230 event rate per year versus the reconstructed energy (a) and zenith (b) of the track selection for a cosmic neutrino flux of $\phi_{\nu_i+\bar{\nu}_i} = 1.2 \cdot 10^{-8} \left(\frac{E_\nu}{\text{GeV}}\right)^{-2}$ GeV^{-1} cm^{-2} s^{-1} sr^{-1}.

4.2 Shower selection

The shower selection aims to improve the sensitivity to point sources and the diffuse neutrino flux by selecting as many neutrino events that not pass the track selection. Events are selected with a shower reconstruction vertex z position below the top layer of optical modules. This is followed by cuts on the number of hits that fulfill the Cherenkov hypothesis. Another boosted decision tree model is trained using variables like reconstructed position, direction, energy, fit quality and the inertia ratio of the hits. Figure 5 shows the KM3NeT/ARCA230 event rate per year versus the reconstructed energy and zenith of the shower selection.
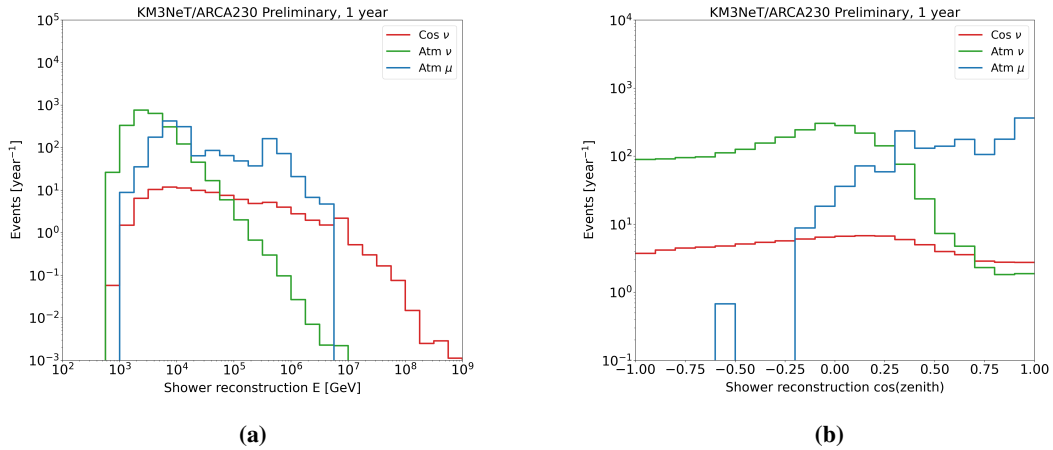

(a)

(b)

Figure 5: Event rates per year versus the reconstructed energy (a) and zenith (b) of the shower selection for a cosmic neutrino flux of $\phi_{\nu_i+\bar{\nu}_i} = 1.2 \cdot 10^{-8} \left(\frac{E_\nu}{\text{GeV}}\right)^{-2}$ GeV^{-1} cm^{-2} s^{-1} sr^{-1}.

4.3 Performance

The effective area of the final selections can be found in figure 6.

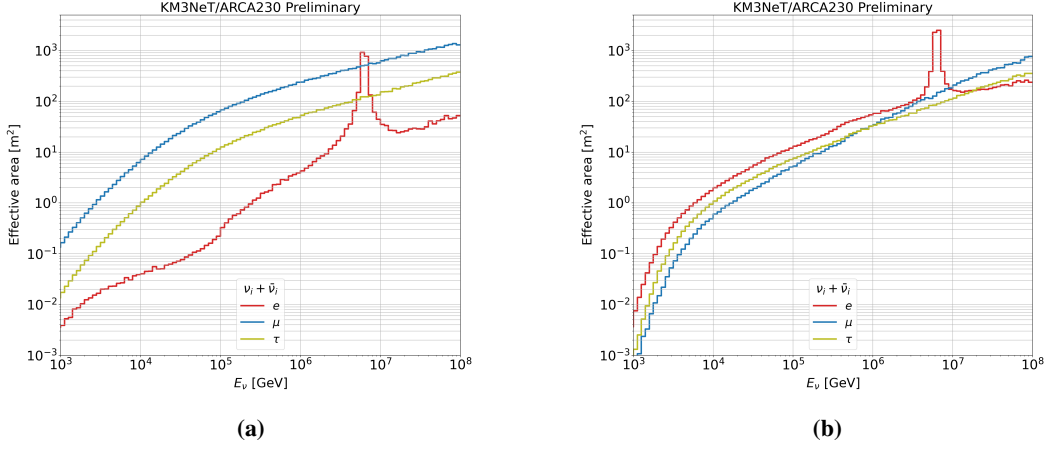**(a)**   **(b)**

Figure 6: Effective area for a flux of $\nu_i + \bar{\nu}_i$ for the track (a) and shower (b) selection for KM3NeT/ARCA230.

The final event rates per year for the full detector are shown in table 1.

	Trigger	Track selection	Shower selection
Atmospheric μ	80.6e6	713	1524
Atmospheric ν	19.1e4	85.2e3	2264
Cosmic ν	728	220	96
Signal efficiency		94.5%	69.7%
Neutrino purity		99%	60.8%

Table 1: Yearly event rate for KM3NeT/ARCA230 at trigger level and for the track and cascade selection for a cosmic neutrino flux of $\phi_{\nu_i + \bar{\nu}_i} = 1.2 \cdot 10^{-8} \left(\frac{E_\nu}{\text{GeV}} \right)^{-2}$ GeV^{-1} cm^{-2} s^{-1} sr^{-1}.

The signal efficiency is calculated by dividing the signal events that pass the selections divided by upgoing signal events for tracks and all signal events for showers. The signal definition for tracks entails events with a muon and that have the direction reconstruction within $10°$. Signal events for showers are events without a muon, that are contained within the detector and have the direction reconstruction within $10°$.

5. Conclusions

This contribution summarises the KM3NeT/ARCA230 reconstruction software and neutrino selections that are used for the current point source and diffuse analyses. The track selection is a pure upgoing neutrino sample and the cascade selection includes as much extra signal as possible. Future improvements will include timing information in the shower reconstruction resulting in an angular resolution below $1°$ above several 100 TeV. A dedicated double shower algorithm and a dedicated neutrino selection is in preparation.

References

[1] Aartsen, M. et al (2013). First observation of PeV-energy neutrinos with IceCube. Physical review letters, 111(2), 021103.

[2] Aartsen, M et al. (2018). Neutrino emission from the direction of the blazar TXS 0506+ 056 prior to the IceCube-170922A alert. Science, 361(6398), 147-151.

[3] Abbasi, R. et al. (2022). Evidence for neutrino emission from the nearby active galaxy NGC 1068. Science, 378(6619), 538-543.

[4] Adrian-Martinez, S. et al. (2016). Letter of intent for KM3NeT 2.0. Journal of Physics G: Nuclear and Particle Physics, 43(8), 084001.

[5] Aiello, S, et al. (2022). The KM3NeT multi-PMT optical module. Journal of Instrumentation, 17(07), P07038.

[6] Aiello, S. et al (2020). gSeaGen: the KM3NeT GENIE-based code for neutrino telescopes. Computer Physics Communications, 256, 107477.

[7] Caiffi, B., Soto, A. G., Heijboer, A., Kulikovskiy, V., Muller, R. S., Sanguineti, M., & KM3NeT Collaboration. (2021). Sensitivity estimates for diffuse, point-like, and extended neutrino sources with KM3NeT/ARCA. Journal of Instrumentation, 16(09), C09030.

[8] Carminati, G., Bazzotti, M., Margiotta, A., & Spurio, M. (2008). Atmospheric MUons from PArametric formulas: a fast GEnerator for neutrino telescopes (MUPAGE). Computer Physics Communications, 179(12), 915-923.

[9] Melis, K. et al. (2017). KM3NeT/ARCA event reconstruction algorithms. In Proceedings, 35th International Cosmic Ray Conference (ICRC2017) (pp. 76-78).

[10] van Eeden, T., Seneca, J. et al. (2022). High-energy reconstruction for single and double cascades using the KM3NeT detector. ICRC2021 arXiv preprint arXiv:2205.02641.

Full Authors List: The KM3NeT Collaboration

S. Aiello^a, A. Albert^{b,bd}, S. Alves Garre^c, Z. Aly^d, A. Ambrosone^{f,e}, F. Ameli^g, M. Andre^h, E. Androutsou^i, M. Anguita^j, L. Aphecetche^k, M. Ardid^l, S. Ardid^l, H. Atmani^m, J. Aublin^n, L. Bailly-Salins^o, Z. Bardačová^{q,p}, B. Baret^n, A. Bariego-Quintana^c, S. Basegmez du Pree^r, Y. Becherini^n, M. Bendahman^{m,n}, F. Benfenati^{t,s}, M. Benhassi^{u,e}, D. M. Benoit^v, E. Berbee^r, V. Bertin^d, S. Biagi^w, M. Boettcher^x, D. Bonanno^w, J. Boumaaza^m, M. Bouta^y, M. Bouwhuis^r, C. Bozza^{z,e}, R.M. Bozza^{f,e}, H.Brânzaş^{aa}, F. Bretaudeau^k, R. Bruijn^{ab,r}, J. Brunner^d, R. Bruno^a, E. Buis^{ac,r}, R. Buompane^{u,e}, J. Busto^d, B. Caiffi^{ad}, D. Calvo^c, S. Campion^{g,ae}, A. Capone^{g,ae}, F. Carenini^{t,s}, V. Carretero^c, T. Cartraud^n, P. Castaldi^{af,s}, V. Cecchini^c, S. Celli^{g,ae}, L. Cerisy^d, M. Chabab^{ag}, M. Chadolias^{ah}, A. Chen^{ai}, S. Cherubini^{aj,w}, T. Chiarusi^s, M. Circella^{ak}, R. Cocimano^w, J. A. B. Coelho^n, A. Coleiro^n, R. Coniglione^w P. Coyle^d, A. Creusot^n, A. Cruz^{al}, G. Cuttone^w, R. Dallier^k, Y. Darras^{ah}, A. De Benedittis^e, B. De Martino^d, V. Decoene^k, R. Del Burgo^e, U.M. Di Cerbo^e, L.S. Di Mauro^w, I. Di Palma^{g,ae}, A.F. Díaz^j, C. Diaz^j, D. Diego-Tortosa^w, C. Distefano^w, A. Domi^{ah}, C. Donzaud^n, D. Dornic^d, M. Dörr^{am}, E. Drakopoulou^i, D. Drouhin^{b,bd}, R. Dvornický^q, T. Eberl^{ah}, E. Eckerová^{q,p}, A. Eddymaoui^m, T. van Eeden^r, M. Eff^n, D. van Eijk^r, I. El Bojaddaini^y, S. El Hedri^n, A. Enzenhöfer^d, G. Ferrara^w, M. D. Filipović^{an}, F. Filippini^{t,s}, D. Franciotti^w, L. A. Fusco^{z,e}, J. Gabriel^{ao}, S. Gagliardini^g, T. Gal^{ah}, J. García Méndez^l, A. Garcia Soto^c, C. Gatius Oliver^r, N. Geißelbrecht^{ah}, H. Ghaddari^y, L. Gialanella^{e,u}, B. K. Gibson^v, E. Giorgio^w, I. Goos^n, D. Goupilliere^o, S. R. Gozzini^c, R. Gracia^{ah}, K. Graf^{ah}, C. Guidi^{ap,ad}, B. Guillon^o, M. Gutiérrez^{aq}, H. van Haren^{ar}, A. Heijboer^r, A. Hekalo^{am}, L. Hennig^{ah}, J. J. Hernández-Rey^c, F. Huang^d, W. Idrissi Ibnsalih^e, G. Illuminati^s, C. W. James^{al}, M. de Jong^{as,r}, P. de Jong^{ab,r}, B. J. Jung^r, P. Kalaczyński^{at,be}, O. Kalekin^{ah}, U. F. Katz^{ah}, N. R. Khan Chowdhury^c, A. Khatun^q, G. Kistauri^{av,au}, C. Kopper^{ah}, A. Kouchner^{aw,n}, V. Kulikovskiy^{ad}, R. Kvatadze^{av}, M. Labalme^o, R. Lahmann^{ah}, G. Larosa^w, C. Lastoria^d, A. Lazo^c, S. Le Stum^d, G. Lehaut^o, E. Leonora^a, N. Lessing^c, G. Levi^{t,s}, M. Lindsey Clark^n, F. Longhitano^a, J. Majumdar^r, L. Malerba^{ad}, F. Mamedov^p, J. Mańczak^c, A. Manfreda^e, M. Marconi^{ap,ad}, A. Margiotta^{t,s}, A. Marinelli^{e,f}, C. Markou^i, L. Martin^k, J. A. Martínez-Mora^l, F. Marzaioli^{u,e}, M. Mastrodicasa^{ae,g}, S. Mastroianni^e, S. Miccichè^w, G. Miele^{f,e}, P. Migliozzi^e, E. Migneco^w, M. L. Mitsou^e, C. M. Mollo^e, L. Morales-Gallegos^{u,e}, C. Morley-Wong^{al}, A. Moussa^y, I. Mozun Mateo^{ay,ax}, R. Muller^r, M. R. Musone^{e,u}, M. Musumeci^w, L. Nauta^r, S. Navas^{aq}, A. Nayerhoda^{ak}, C. A. Nicolau^g, B. Nkosi^{ai}, B. Ó Fearraigh^{ab,r}, V. Oliviero^{f,e}, A. Orlando^w, E. Oukacha^n, D. Paesani^w, J. Palacios González^c, G. Papalashvili^{au}, V. Parisi^{ap,ad}, E.J. Pastor Gomez^c, A. M. Păun^{aa}, G. E. Păvălaş^{aa}, S. Peña Martínez^n, M. Perrin-Terrin^d, J. Perronnel^o, V. Pestel^{ay}, R. Pestes^n, P. Piattelli^w, C. Poirè^{z,e}, V. Popa^{aa}, T. Pradier^b, S. Pulvirenti^w, G. Quéméner^o, C. Quiroz^l, U. Rahaman^c, N. Randazzo^a, R. Randriatoamanana^k, S. Razzaque^{az}, I.C. Rea^e, D. Real^c, S. Reck^{ah}, G. Riccobene^w, J. Robinson^x, A. Romanov^{ap,ad}, A. Šaina^c, F. Salesa Greus^c, D. F. E. Samtleben^{as,r}, A. Sánchez Losa^{c,ak}, S. Sanfilippo^w, M. Sanguineti^{ap,ad}, C. Santonastaso^{ba,e}, D. Santonocito^w, P. Sapienza^w, J. Schnabel^{ah}, J. Schumann^{ah}, H. M. Schutte^x, J. Seneca^r, N. Sennan^y, B. Setter^{ah}, I. Sgura^{ak}, R. Shanidze^{au}, Y. Shitov^p, F. Šimkovic^q, A. Simonelli^e, A. Sinopoulou^a, M.V. Smirnov^{ah}, B. Spisso^e, M. Spurio^{t,s}, D. Stavropoulos^i, I. Štekl^p, M. Taiuti^{ap,ad}, Y. Tayalati^m, H. Tedjditi^d, H. Thiersen^x, I. Tosta e Melo^{a,aj}, B. Trocmé^n, V. Tsourapis^i, E. Tzamariudaki^i, A. Vacheret^o, V. Valsecchi^w, V. Van Elewyck^{aw,n}, G. Vannoye^d, G. Vasileiadis^{bb}, F. Vazquez de Sola^r, C. Verilhac^n, A. Veutro^{g,ae}, S. Viola^w, D. Vivolo^{u,e}, J. Wilms^{bc}, E. de Wolf^{ab,r}, H. Yepes-Ramirez^l, G. Zarpapis^i, S. Zavatarelli^{ad}, A. Zegarelli^{g,ae}, D. Zito^w, J. D. Zornoza^c, J. Zúñiga^c, and N. Zywucka^x.

^{a}INFN, Sezione di Catania, Via Santa Sofia 64, Catania, 95123 Italy

^{b}Université de Strasbourg, CNRS, IPHC UMR 7178, F-67000 Strasbourg, France

^{c}IFIC - Instituto de Física Corpuscular (CSIC - Universitat de València), c/Catedrático José Beltrán, 2, 46980 Paterna, Valencia, Spain

^{d}Aix Marseille Univ, CNRS/IN2P3, CPPM, Marseille, France

^{e}INFN, Sezione di Napoli, Complesso Universitario di Monte S. Angelo, Via Cintia ed. G, Napoli, 80126 Italy

^{f}Università di Napoli "Federico II", Dip. Scienze Fisiche "E. Pancini", Complesso Universitario di Monte S. Angelo, Via Cintia ed. G, Napoli, 80126 Italy

^{g}INFN, Sezione di Roma, Piazzale Aldo Moro 2, Roma, 00185 Italy

^{h}Universitat Politècnica de Catalunya, Laboratori d'Aplicacions Bioacústiques, Centre Tecnològic de Vilanova i la Geltrú, Avda. Rambla Exposició, s/n, Vilanova i la Geltrú, 08800 Spain

^{i}NCSR Demokritos, Institute of Nuclear and Particle Physics, Ag. Paraskevi Attikis, Athens, 15310 Greece

^{j}University of Granada, Dept. of Computer Architecture and Technology/CITIC, 18071 Granada, Spain

^{k}Subatech, IMT Atlantique, IN2P3-CNRS, Université de Nantes, 4 rue Alfred Kastler - La Chantrerie, Nantes, BP 20722 44307 France

^{l}Universitat Politècnica de València, Instituto de Investigación para la Gestión Integrada de las Zonas Costeras, C/ Paranimf, 1, Gandia, 46730 Spain

^{m}University Mohammed V in Rabat, Faculty of Sciences, 4 av. Ibn Battouta, B.P. 1014, R.P. 10000 Rabat, Morocco

^{n}Université Paris Cité, CNRS, Astroparticule et Cosmologie, F-75013 Paris, France

^{o}LPC CAEN, Normandie Univ, ENSICAEN, UNICAEN, CNRS/IN2P3, 6 boulevard Maréchal Juin, Caen, 14050 France

^{p}Czech Technical University in Prague, Institute of Experimental and Applied Physics, Husova 240/5, Prague, 110 00 Czech Republic

^{q}Comenius University in Bratislava, Department of Nuclear Physics and Biophysics, Mlynska dolina F1, Bratislava, 842 48 Slovak Republic

^{r}Nikhef, National Institute for Subatomic Physics, PO Box 41882, Amsterdam, 1009 DB Netherlands

^{s}INFN, Sezione di Bologna, v.le C. Berti-Pichat, 6/2, Bologna, 40127 Italy

^{t}Università di Bologna, Dipartimento di Fisica e Astronomia, v.le C. Berti-Pichat, 6/2, Bologna, 40127 Italy

^{u}Università degli Studi della Campania "Luigi Vanvitelli", Dipartimento di Matematica e Fisica, viale Lincoln 5, Caserta, 81100 Italy

^{v}E. A. Milne Centre for Astrophysics, University of Hull, Hull, HU6 7RX, United Kingdom

[w] INFN, Laboratori Nazionali del Sud, Via S. Sofia 62, Catania, 95123 Italy

[x] North-West University, Centre for Space Research, Private Bag X6001, Potchefstroom, 2520 South Africa

[y] University Mohammed I, Faculty of Sciences, BV Mohammed VI, B.P. 717, R.P. 60000 Oujda, Morocco

[z] Università di Salerno e INFN Gruppo Collegato di Salerno, Dipartimento di Fisica, Via Giovanni Paolo II 132, Fisciano, 84084 Italy

[aa] ISS, Atomistilor 409, Măgurele, RO-077125 Romania

[ab] University of Amsterdam, Institute of Physics/IHEF, PO Box 94216, Amsterdam, 1090 GE Netherlands

[ac] TNO, Technical Sciences, PO Box 155, Delft, 2600 AD Netherlands

[ad] INFN, Sezione di Genova, Via Dodecaneso 33, Genova, 16146 Italy

[ae] Università La Sapienza, Dipartimento di Fisica, Piazzale Aldo Moro 2, Roma, 00185 Italy

[af] Università di Bologna, Dipartimento di Ingegneria dell'Energia Elettrica e dell'Informazione "Guglielmo Marconi", Via dell'Università 50, Cesena, 47521 Italia

[ag] Cadi Ayyad University, Physics Department, Faculty of Science Semlalia, Av. My Abdellah, P.O.B. 2390, Marrakech, 40000 Morocco

[ah] Friedrich-Alexander-Universität Erlangen-Nürnberg (FAU), Erlangen Centre for Astroparticle Physics, Nikolaus-Fiebiger-Straße 2, 91058 Erlangen, Germany

[ai] University of the Witwatersrand, School of Physics, Private Bag 3, Johannesburg, Wits 2050 South Africa

[aj] Università di Catania, Dipartimento di Fisica e Astronomia "Ettore Majorana", Via Santa Sofia 64, Catania, 95123 Italy

[ak] INFN, Sezione di Bari, via Orabona, 4, Bari, 70125 Italy

[al] International Centre for Radio Astronomy Research, Curtin University, Bentley, WA 6102, Australia

[am] University Würzburg, Emil-Fischer-Straße 31, Würzburg, 97074 Germany

[an] Western Sydney University, School of Computing, Engineering and Mathematics, Locked Bag 1797, Penrith, NSW 2751 Australia

[ao] IN2P3, LPC, Campus des Cézeaux 24, avenue des Landais BP 80026, Aubière Cedex, 63171 France

[ap] Università di Genova, Via Dodecaneso 33, Genova, 16146 Italy

[aq] University of Granada, Dpto. de Física Teórica y del Cosmos & C.A.F.P.E., 18071 Granada, Spain

[ar] NIOZ (Royal Netherlands Institute for Sea Research), PO Box 59, Den Burg, Texel, 1790 AB, the Netherlands

[as] Leiden University, Leiden Institute of Physics, PO Box 9504, Leiden, 2300 RA Netherlands

[at] National Centre for Nuclear Research, 02-093 Warsaw, Poland

[au] Tbilisi State University, Department of Physics, 3, Chavchavadze Ave., Tbilisi, 0179 Georgia

[av] The University of Georgia, Institute of Physics, Kostava str. 77, Tbilisi, 0171 Georgia

[aw] Institut Universitaire de France, 1 rue Descartes, Paris, 75005 France

[ax] IN2P3, 3, Rue Michel-Ange, Paris 16, 75794 France

[ay] LPC, Campus des Cézeaux 24, avenue des Landais BP 80026, Aubière Cedex, 63171 France

[az] University of Johannesburg, Department Physics, PO Box 524, Auckland Park, 2006 South Africa

[ba] Università degli Studi della Campania "Luigi Vanvitelli", CAPACITY, Laboratorio CIRCE - Dip. Di Matematica e Fisica - Viale Carlo III di Borbone 153, San Nicola La Strada, 81020 Italy

[bb] Laboratoire Univers et Particules de Montpellier, Place Eugène Bataillon - CC 72, Montpellier Cédex 05, 34095 France

[bc] Friedrich-Alexander-Universität Erlangen-Nürnberg (FAU), Remeis Sternwarte, Sternwartstraße 7, 96049 Bamberg, Germany

[bd] Université de Haute Alsace, rue des Frères Lumière, 68093 Mulhouse Cedex, France

[be] AstroCeNT, Nicolaus Copernicus Astronomical Center, Polish Academy of Sciences, Rektorska 4, Warsaw, 00-614 Poland

Acknowledgements